[DRAFT] Proceedings of the Eurohaptics 2018, pp 209-220, June 13-16, Pisa, Italy.

Haptic Tracing of Midair Linear Trajectories Presented by Ultrasound Bessel Beams

Shun Suzuki, Keisuke Hasegawa, Yasutoshi Makino, and Hiroyuki Shinoda.

The University of Tokyo, 5-1-5 Kashiwanoha, Kashiwa-shi, Chiba-ken 277-8561,
suzuki@hapis.k.u-tokyo.ac.jp, Keisuke_Hasegawa@ipc.i.u-tokyo.ac.jp, {Yasutoshi_Makino,Hiroyuki_Shinoda}@k.u-tokyo.ac.jp

Abstract. This paper verifies the ability of human subjects with no audiovisual clues to trace their hands along an invisible vibrotactile line in three-dimensional space created by an ultrasound Bessel beam. A narrow, long, and stationary Bessel beam that passes through a target position is generated. The beam produces midair vibrotactile stimuli on the subjects' hands. The subjects are required to perceive the beam location and direction actively to trace the presented linear trajectory. With our method, no real-time hand tracking is necessary, which guarantees no latency in presenting the vibrotactile stimuli. We experimentally verified that the subjects were able to trace the beam over 50 cm in its stretching direction with their hands. The average deviation from the beam center was less than 6 cm. Unlike conventional wearable-based motion guidance, the proposed technique requires no devices to be worn by the users in practical situations.

1 Introduction

In this paper, we verify the haptic tracing ability of a hand along an invisible line created by ultrasound; that is, we examine whether a human being can move his/her hand along a narrow ultrasound Bessel beam by perceiving the vibration caused by the beam. An ultrasound phased array can produce various types of localized sound fields as well as the single or multiple focusing beams seen in many midair haptic systems [1–3]. A Bessel beam, which is a one-dimensional long narrow beam, is a typical example of such a computer-designed ultrasound field. Recent research confirmed successful beam generation in midair and referred to the possibility of its application in air stream control [4]. As with the focusing beams mentioned above, such a Bessel beam is perceivable by the hands and fingers, which suggests the possibility of non-contact motion guidance that leads a hand to a target along the beam as shown in Fig. 1. The motivation of this study was that it was fairly easy for the authors to follow a Bessel beam under certain conditions.

Suppose you are surrounded by devices with many functions. If you are a surgeon in an operating room, there must be various kinds of surgical tools around you. In such a situation, a non-contact motion guidance enables to lead the surgeon's hand to the necessary tool without any human assistant who hands over the tool. Such a tool might be replaced with an optically-created virtual volume knob or dial in a future car. In order for a driver to operate the devices without relying on vision, he/she must remember the arrangement of the interface. Non-contact motion guidance can lead the driver's hand to the virtual dials before remembering the locations. The goal of this paper is to verify how efficiently the beam leads the user's hand to the target point under consideration for such applications.

Many studies have been conducted on motion guidance by wearable haptic devices. These studies are based on pseudo attraction force [5], torque stimuli [6, 7], and vibrators attached to the waist or arms [8, 9]. In [10], direction was given by the vibration of a mobile handheld device while swinging the hand horizontally. The display of a virtual curving handrail to the hand [11] and other deforming devices [12–14] were also proposed. These methods guide motion by providing vibrotactile/kinesthetic stimuli to the human body. This approach is typically applicable to pedestrian navigation.

This paper focuses on the traceability of a stationary Bessel beam shorter than 1 m, where the user actively perceives the beam location and direction. The first obvious difference from wearable-based motion guidance is that no devices are required by the user. The second difference is that the Bessel beam is a spatially-extending stationary stimulus, requiring no real-time hand tracking. This guarantees no latency in the presentation of the vibrotactile stimuli. In the proposed system, a user searches for the stationary beam actively just as one would follow handrails.

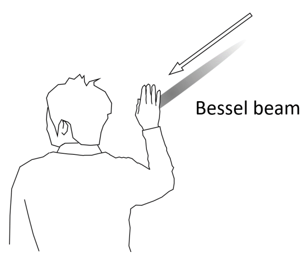

Fig. 1. Subject can trace the Bessel beam without looking.

2 Airborne Ultrasound Tactile Display (AUTD)

Midair haptics using Airborne Ultrasound Tactile Display (AUTD), as proposed in [15], provide noncontact tactile feedback to the surface of a human body. Such midair haptics along with wearable haptics are promising options to provide haptic feedback in three-dimensional (3D) interfaces. The advantage of midair haptics in an air flow device [16] is that no devices are required to be worn by the user. Using AUTD, the stimulation position can be freely and precisely determined at arbitrary times with the focal amplitude modulation creating arbitrary temporal force patterns in the workspace.

AUTD is realized by a phased array in which ultrasonic transducers are typically arranged in a lattice pattern [1–3]. Not only the focusing beam used in previous studies, the phased array can also create a narrow and long ultrasound Bessel beam by controlling the phases of the transducers. Figure 2 shows a photograph and design drawing of the AUTD used in this study. Since a multiunit AUTD system with a widened aperture can broaden the workspace [17], nine AUTD subunits were fixed to an aluminum frame. One AUTD subunit has 249 transducers and overall, the AUTD has 2241 transducers. A depth sensor (Kinect II, Microsoft Corp.) was also fixed to the frame.

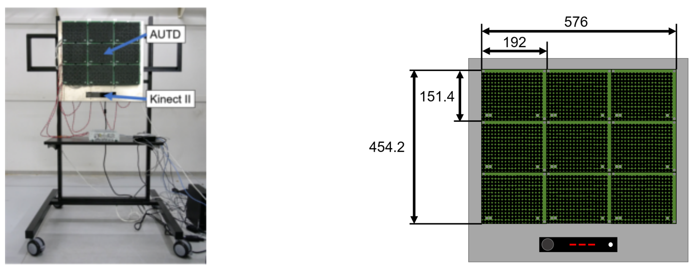

Fig. 2. (Left) Photograph and (Right) drawing of AUTD. Dimensions are in mm.

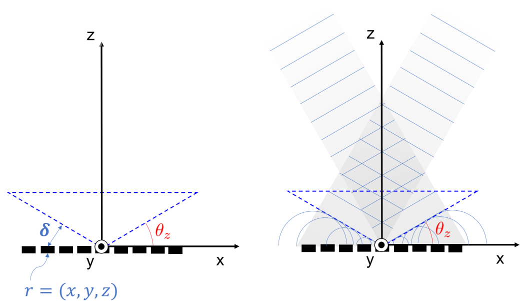

Fig. 3. Generation of the Bessel beam by virtual cone-shaped sound source.

A Bessel beam is generated by conical wavefronts [4]. Figure 3 is a schematic diagram of a Bessel beam generated with an array of sound sources. Each transducer has a phase shift that is proportional to the distance between its position $\boldsymbol{r} = (x, y, z)$ and the cone-shaped virtual sound source. Suppose that the origin is located at the vertex of the cone, the z axis is identical to that of the cone with its direction oriented towards the bottom, and θ_z is the angle between the side of the cone and the x-y plane. Here, a proper phase shift $\delta(\boldsymbol{r})$ is given by

$$\delta(\boldsymbol{r}) = k(\sqrt{x^2 + y^2} \sin\theta_z - z\cos\theta_z) \tag{1}$$

where k denotes the ultrasound wavelength. The beam length L is roughly given by

$$L = \frac{A}{2\tan\theta_z} \tag{2}$$

where A is the array aperture. In this paper, we set the value of θ_z to $13°$.

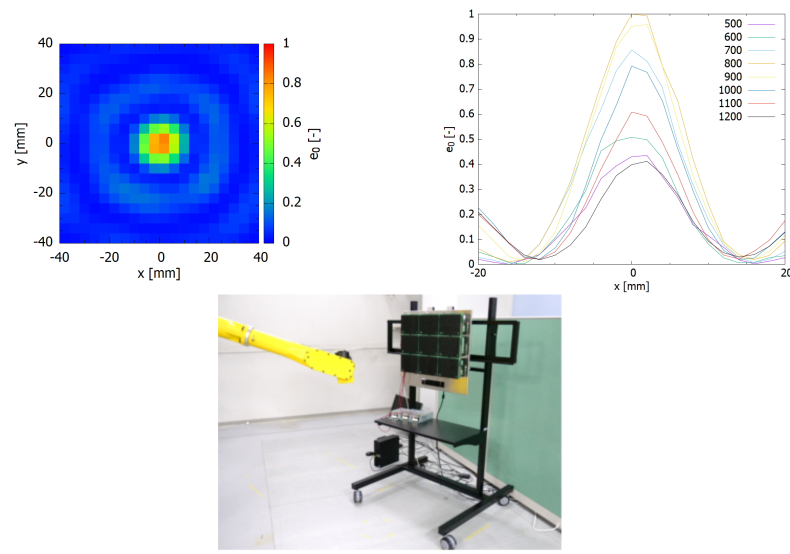

Fig. 4. Experimental results of the acoustic energy-density measurement. Left: Cross section of the Bessel beam at $z = 800$ mm. Right: Normalized acoustic energy density at $(x, 0, z)$ for $z = 500$ mm to 1200 mm. The maximum acoustic energy density was $107\,\mathrm{J/m^3}$, where the normalized value is 1. Bottom: Measurement setup. A microphone was attached to the tip of the yellow robot arm.

Figure 4 shows the experimental results of the acoustic energy-density measurement. The normalized acoustic energy density of the Bessel beam in the experiment was measured by a microphone attached to a scanning robot arm as shown in the bottom photo of Fig. 4. We use a coordinate system with its origin located at the center of the phased-array surface. The x and y axes are parallel to the long and the short sides of the phased array, respectively. The z axis is perpendicular to the phased-array surface, forming the right-hand system (shown in Fig. 6). The cross section of the beam becomes concentric, and the intensity of the Bessel beam in the cross section is described by the Bessel function of the first kind. As shown in Fig. 4, the ultrasound Bessel beam used in this experiment was concentric and kept a constant radius from $z = 500$ mm to 1200 mm.

3 Tracing Experiments

In this experiment, to verify the haptic traceability of an invisible line, we generated an acoustic Bessel beam of 40 kHz ultrasound and examined whether a hand could trace the beam. During this experiment, the position of the Bessel beam was fixed. The radiation pressure was modulated with a 150 Hz sinusoidal wave.

We performed two experiments. In Experiment 1, the Bessel beam was directed at a participant's hand. We then examined whether the participants could perceive it by asking them to estimate the beam direction while they moved their hands along the Bessel beam. In Experiment 2, we investigated the influence of training.

Six men in their twenties participated in these experiments.

3.1 Experiment 1

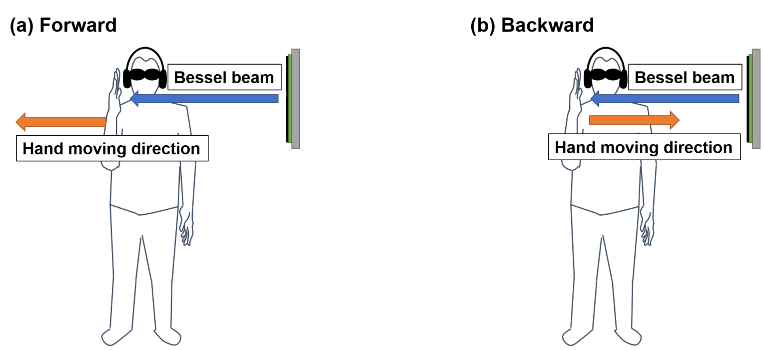

Fig. 5. Participants were instructed to move their hands in the (a) forward or (b) backward direction of the Bessel beam.

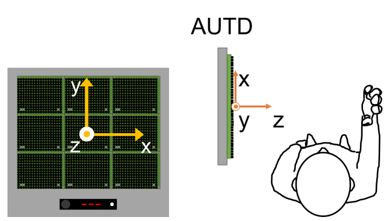

Fig. 6. Coordinate system.

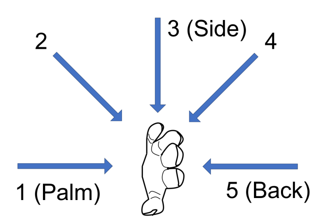

Fig. 7. The hand was irradiated from five directions.

Procedure In this experiment, the right hand of a participant was irradiated by a Bessel beam. A schematic diagram of the experiment is shown in Fig. 5, and the coordinate system is shown in Fig. 6. The hand was irradiated from five directions as shown in Fig. 7.

The Bessel beam direction was fixed throughout the experiment, and the direction and position of the participant was changed by the experimenter. The participants wore eye-masks and headphones playing pink noise. The initial positions and orientations of the participants were reset in each trial of the experiment to ensure that each trial was independent from the previous trials.

The participant's hand was guided to a fixed position $(x, y, z) = (0, 0, 60\,\mathrm{cm})$. The participant was then guided to put his hand in front of his body with his fingers up and his palm orthogonal to his chest, as shown in Fig. 6. The participants were instructed to keep their hand still until they felt the beam vibration. After perceiving the beam, participants moved their hands forward along the beam. During this movement, they were allowed to change the direction of their hands freely. We observed the trajectory of the hand up to $(x, y, z) = (0, 0, 110\,\mathrm{cm})$ using a depth sensor (Kinect II, Microsoft Corp.). Each participant underwent five trials corresponding to each of the five directions illustrated in Fig. 7. The order in which the directions were selected was random for each participant.

We conducted another experiment in which the direction of hand movement was reversed, i.e., "backward." The experimenter placed the participant's hand at $(x, y, z) = (0, 0, 110\,\mathrm{cm})$ and instructed the participant to move his hand in the direction opposite of the beam direction. We then observed the movement of the hand to $(x, y, z) = (0, 0, 60\,\mathrm{cm})$. As before, there were five trials for each participant in these experiments.

Note that in both experiments there was no measurement of the participants' hand positions. The aim of the experiments was not to provide accurate stimulation that tracks user position but to investigate human performance in the haptic tracing of immobilized midair ultrasound beams.

Result Table. 1 shows the arrival rates, which are defined as the ratio of participant whose hand reached $z = 110\,\mathrm{cm}$ (forward) or $z = 60\,\mathrm{cm}$ (backward) within 20 seconds after the Bessel beam irradiation. We define deviation ε and average speed v as

$$\varepsilon = \frac{1}{N}\sum_{i=1}^{N}\sqrt{x_i^2 + y_i^2} \tag{3}$$

$$v = \frac{|\boldsymbol{x}_N - \boldsymbol{x}_1|}{t} \tag{4}$$

where $\{\boldsymbol{x}_i = (x_i, y_i, z_i)\}_{i=1,2,\ldots,N}$ are the sampled points in the captured trajectories of the hands from the start to the goal, and t is the total elapsed time of the trial. These quantities are calculated for each trial. As seen in Fig. 4, the energy distribution of a Bessel beam is a set of concentric rings, where the central part is perceived most strongly. We clarify here that according to the above definition, ε represents the average deviation from the central line of the beam.

The values of ε and v for each participant from a to f are shown in Fig. 8 and 9, respectively. The averages and standard deviations shown in Fig. 8 and 9 were calculated only for the participants who arrived at the goal. Figures 10 and 11 show the hand trajectories for the forward and backward cases, respectively.

Table 1. Experimental results of Arrival rate.

	Direction.				
	1 (Palm)	2	3 (side)	4	5 (back)
Forward	0.83	0.67	0.33	0.17	0.17
Backward	1	1	0.67	0.5	0.67

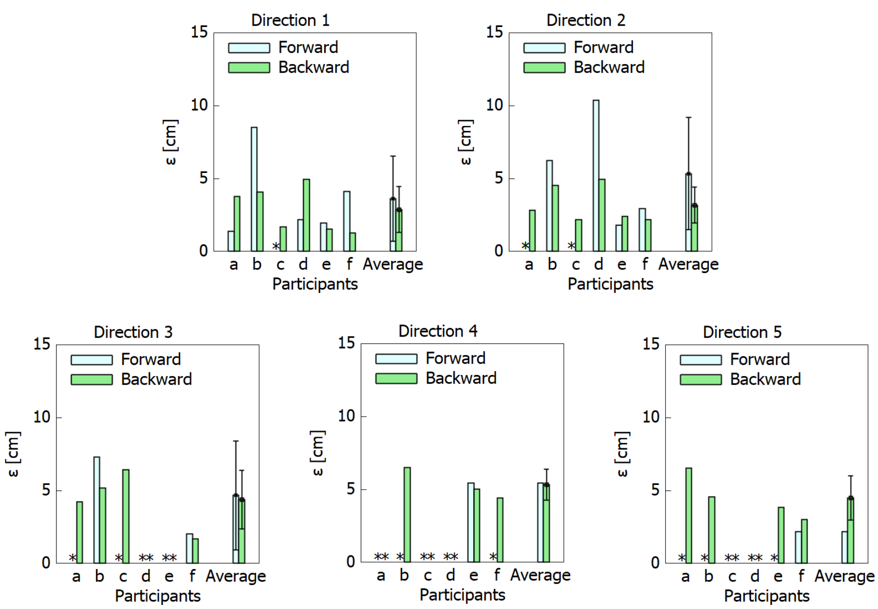

Fig. 8. Hand position deviations from the center of the Bessel beam for the directions from 1 to 5 and the six subjects from a to f. The beam directions are shown in Fig. 7. The asterisk represents cases in which the hand did not arrive at the goal. These cases are excluded from the average.

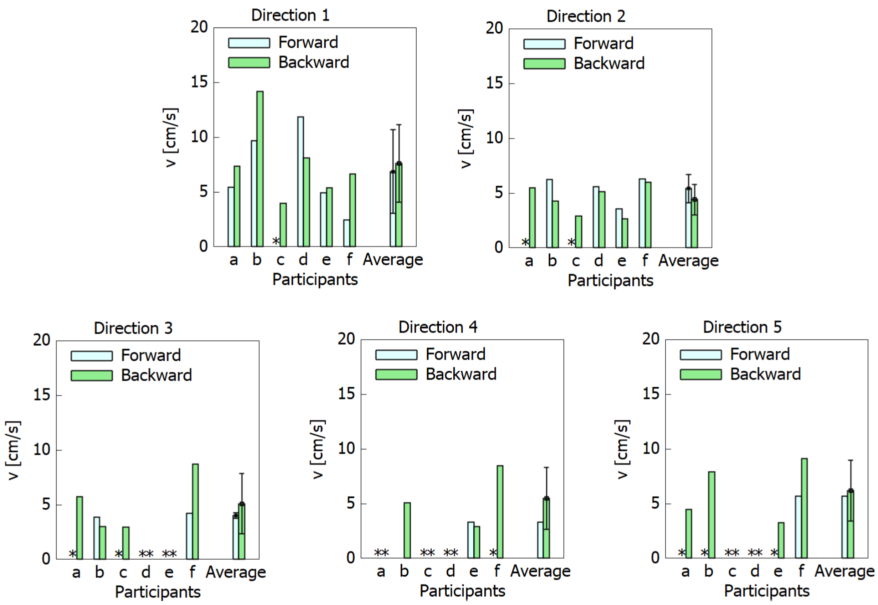

Fig. 9. Speeds of hand tracing for a 50 cm moving distance. The Bessel beam direction is shown in Fig. 7. The asterisk represents cases in which the hand did not arrive at the goal. These cases are excluded from the average.

Discussion The results show that all of the participants could follow the Bessel beam backwards for beam Direction 1 irradiating the palm perpendicularly. This was the easiest case and the participants were able to reach the goal.

The forward case seemed more difficult than the backward case. For all beam directions, the arrival rates in the backward case were higher than those in the forward case, and there was a significant difference in the p-value of 3.2×10^{-3} in the t-test. This tendency is also observed in Fig. 10 and 11. With respect to the Direction 1 cases, there was one participant who lost track of the beam once (shown as the green line) in the forward case, but this did not happen for the backward case. Some subjects experienced difficulty with Directions 3, 4, and 5 where the hand was irradiated from the side or the back. This is because the tactile perception of the weak vibration on the side and the back of the hand was too weak to notice the tactile stimulus.

It should be noted that the Bessel beam was accompanied by an acoustic stream and the participants reported that they felt a wind most strongly at $(x, y, z) = (0, 0, 110\,\text{cm})$. The acoustic stream, felt as a wind, was an additional cue to determine the beam direction. In the backwards case, the participants felt this acoustic stream most strongly at the initial position. It is thought that this made the decision regarding the motion direction easier, which led to better results for the backward case than for the forward case. In summary, it can

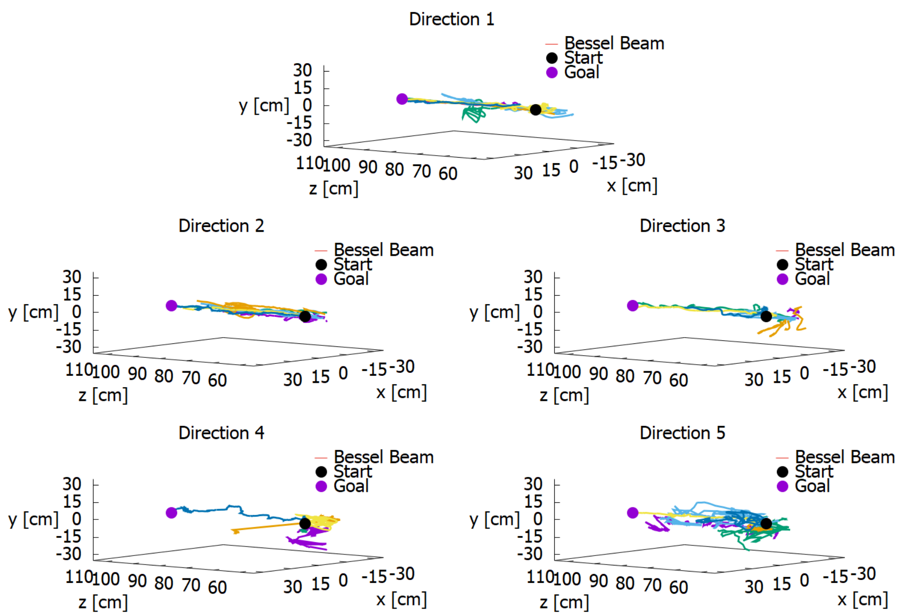

Fig. 10. Hand trajectories of forward motion. The Bessel beam direction is shown in Fig. 7.

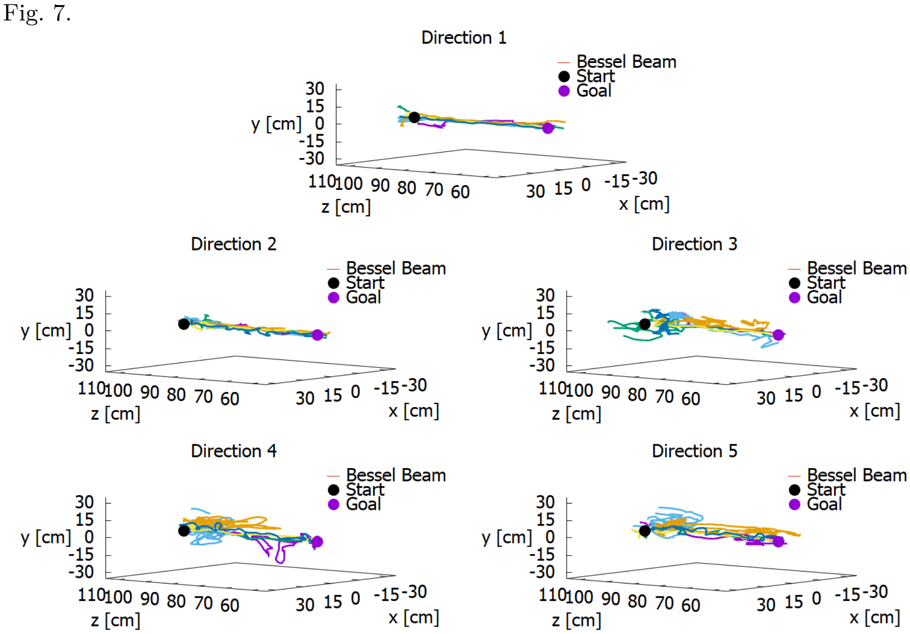

Fig. 11. Hand trajectories of Backward motion. The Bessel beam direction is shown in Fig. 7.

safely be concluded that it is easy for the palm to follow the beam in a backwards direction while difficulty arises when the hand or the tracing direction is reversed.

3.2 Experiment 2

In order to investigate the effect of training, the same procedure as Experiment 1 was repeated four times for Directions 2 and 3. As shown in the results of Experiment 1, it was easy for almost every participant to reach the goal in the case of Direction 1. In the cases of Directions 3 and 4, it seemed to be difficult to even perceive the stimulus. Hence, we chose Direction 2 and 3 to investigate the effect of training regarding moving the hand along the Bessel beam on the arrival rate, speed, and deviation.

Procedure The experiment procedure was the same as that of Experiment 1. However, the beam direction was limited to Directions 2 and 3, and the participants were not informed of this.

Result The arrival rates for each trial number are shown in Fig. 12, and the averages of ε and v are also shown in Fig. 12, where the non-traceable cases are excluded from the averages. We define the trial number as the sequential order of the trial. Note that trial number 1 corresponds to the result of Experiment 1.

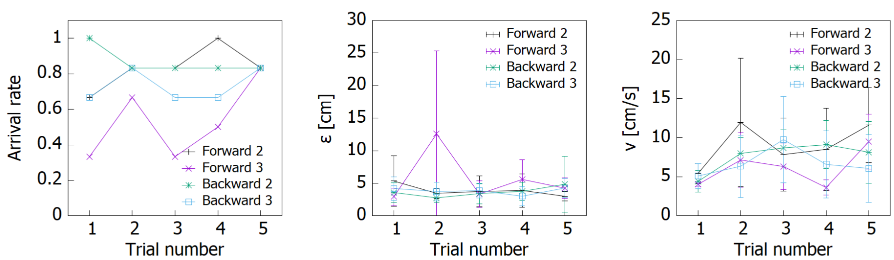

Fig. 12. (Left) Arrival rate, (Middle) deviation ε and (Right) speed v vs. trial number.

Discussion Under the condition of forward movement and beam Direction 3, there was a significant difference in the participant-averaged arrival rate between the first trial and the fifth trial with a p-value of 0.038. There was no statistically significant difference in arrival rate under other conditions. As shown in Fig. 12, the value of ε hardly changed, and it was approximately 5 cm. On the other hand, under the condition of the forward motion, significant differences were seen in v between the first trial and the fifth trial with a p-value of 0.021 and 0.012 for Directions 2 and 3, respectively. There was no statistically significant difference in v for backward motion. These results suggest that haptic tracing ability could be improved with a short period of training, even for the relatively difficult forward-Direction-3 case.

4 Conclusion

In this paper, we evaluated the haptic tracing ability of a hand along an ultrasound Bessel beam. We confirmed that a human being could move his bare hand along the ultrasound Bessel beam without visual and auditory information, and without wearing any devices. More specifically, we experimentally revealed that it was easy to follow the beam by hand, with the palm facing the beam flow.

In the experiment, the average deviation from the center of the Bessel beam was less than 6 cm for all of the experimental conditions, excluding the data for the non-traceable (failed arrival) cases. This is almost the same size as the palm. Thus, it can be said that participants were able to clearly perceive and trace the Bessel beam. The average hand movement speed along the beam was approximately 5 cm/s, which might seem fast enough for real-life situations. However, this value is not the limit of the tracing speed for the airborne tactile stimulus of the human hand. The speed differed greatly among participants and the minimum value was 2.6 cm/s, while the maximum was 14.1 cm/s. This range was as a result of the lack of instruction regarding the movement speed. We expect that the speed can be increased with practice.

The Bessel beam used in this paper is a straight line, and the direction of the hand guidance is limited to one dimension. Additionally, under our experimental setup, the guidance distance was limited to approximately 50 cm. Verification of the tracing ability for a longer-distance airborne tactile stimulus line and bent lines remains as a future study.

Acknowledgements. This work was partly supported by JSPS KAKENHI Grant Number JP15H05316 and JP16H06303.

References

1. Hoshi, T., Takahashi, M., Iwamoto, T., Shinoda, H.: Noncontact tactile display based on radiation pressure of airborne ultrasound. IEEE Transactions on Haptics 3(3), 155–165 (July 2010)
2. Carter, T., Seah, S.A., Long, B., Drinkwater, B., Subramanian, S.: Ultrahaptics: Multi-point mid-air haptic feedback for touch surfaces. In: Proceedings of the 26th Annual ACM Symposium on User Interface Software and Technology. pp. 505–514. UIST '13, ACM, New York, NY, USA (2013), http://doi.acm.org/10.1145/2501988.2502018
3. Korres, G., Eid, M.: Haptogram: Ultrasonic point-cloud tactile stimulation. IEEE Access 4, 7758–7769 (2016)
4. Hasegawa, K., Qiu, L., Noda, A., Inoue, S., Shinoda, H.: Electronically steerable ultrasound-driven long narrow air stream. Applied Physics Letters 111(6), 064104 (2017), https://doi.org/10.1063/1.4985159

5. Amemiya, T., Ando, H., Maeda, T.: Lead-me interface for a pulling sensation from hand-held devices. ACM Trans. Appl. Percept. 5(3), 15:1–15:17 (Sep 2008), http://doi.acm.org/10.1145/1402236.1402239
6. Choiniere, J.P., Gosselin, C.: Development and experimental validation of a haptic compass based on asymmetric torque stimuli. IEEE transactions on haptics 10(1), 29–39 (2017)
7. Walker, J., Culbertson, H., Raitor, M., Okamura, A.: Haptic orientation guidance using two parallel double-gimbal control moment gyroscopes. IEEE Transactions on Haptics PP(99), 1–1 (2017)
8. Cosgun, A., Sisbot, E.A., Christensen, H.I.: Guidance for human navigation using a vibro-tactile belt interface and robot-like motion planning. In: 2014 IEEE International Conference on Robotics and Automation (ICRA). pp. 6350–6355 (May 2014)
9. Baldi, T.L., Scheggi, S., Aggravi, M., Prattichizzo, D.: Haptic guidance in dynamic environments using optimal reciprocal collision avoidance. IEEE Robotics and Automation Letters 3(1), 265–272 (Jan 2018)
10. Kawaguchi, H., Nojima, T.: Stravigation: a vibrotactile mobile navigation for exploration-like sightseeing. In: Advances in Computer Entertainment, pp. 517–520. Springer (2012)
11. Imamura, Y., Arakawa, H., Kamuro, S., Minamizawa, K., Tachi, S.: HAPMAP: Haptic walking navigation system with support by the sense of handrail (2011)
12. Frey, M.: Cabboots: shoes with integrated guidance system. In: Proceedings of the 1st international conference on Tangible and embedded interaction. pp. 245–246. ACM (2007)
13. Hemmert, F., Hamann, S., Löwe, M., Wohlauf, A., Zeipelt, J., Joost, G.: Take me by the hand: haptic compasses in mobile devices through shape change and weight shift. In: Proceedings of the 6th Nordic Conference on Human-Computer Interaction: Extending Boundaries. pp. 671–674. ACM (2010)
14. Spiers, A.J., Dollar, A.M.: Design and evaluation of shape-changing haptic interfaces for pedestrian navigation assistance. IEEE Transactions on Haptics 10(1), 17–28 (Jan 2017)
15. Iwamoto, T., Tatezono, M., Shinoda, H.: Non-contact method for producing tactile sensation using airborne ultrasound. Haptics: Perception, Devices and Scenarios pp. 504–513 (2008)
16. Sodhi, R., Poupyrev, I., Glisson, M., Israr, A.: Aireal: interactive tactile experiences in free air. ACM Transactions on Graphics (TOG) 32(4), 134 (2013)
17. Hasegawa, K., Shinoda, H.: Aerial vibrotactile display based on multiunit ultrasound phased array. IEEE Transactions on Haptics pp. 1–1 (2018), http://doi.org/10.1109/TOH.2018.2799220